

# Use of Noninvasive Imaging in Cardiac Amyloidosis

Raymundo Alain Quintana-Quezada, MD  
Syed Wamique Yusuf, MD  
Jose Banchs, MD\*

## Address

\*Department of Cardiology, The University of Texas MD Anderson Cancer Center,  
1515 Holcombe Blvd. Unit 1451, Houston, TX, 77030, USA  
Email: jbanchs@mdanderson.org

Published online: 16 May 2016

© Springer Science+Business Media New York 2016

This article is part of the Topical Collection on *Cardio-oncology*

**Keywords** Cardiac amyloidosis · Cardiac magnetic resonance · Endomyocardial biopsy · Cardio-oncology

**Abbreviations** *AL* Light chain amyloidosis · *ATTR* Transthyretin amyloidosis · *CA* Cardiac amyloidosis · *LV* Left ventricle · *PSIR* Phase-sensitive inversion recovery · *MACE* Major adverse cardiac event · *HFpEF* Heart failure with preserved ejection fraction

## Opinion statement

Cardiac involvement in amyloidosis is associated with poor outcomes. The standard test for the diagnosis of cardiac amyloidosis is endomyocardial biopsy but given current advances in noninvasive imaging, the diagnosis is frequently obtained or strongly suspected without biopsy. Echocardiography is the most utilized cardiac imaging modality, particularly myocardial strain measures with this modality have been found to be a predictor of clinical outcomes, superior to traditional parameters. Other known imaging modalities with new, useful protocols for this pathology include nuclear imaging and cardiac magnetic resonance (CMR). In particular, CMR has excellent sensitivity and specificity.

## Introduction

Amyloidosis is a rare disease caused by the deposition of misfolded  $\beta$ -pleated fibrils in tissues and organs leading to dysfunction by multiple mechanisms [1•, 2–6]. So far, 31 different types of amyloid fibril proteins have been described in humans; and up to six types of amyloid fibril proteins can affect the heart [7•]. Light chain (AL) and transthyretin (ATTR) amyloidosis are the two

most prevalent and studied types in cardiac amyloidosis. The annual incidence rate of AL amyloidosis is estimated to be nine per million person-years, and [8, 9] cardiac involvement takes place in over 50 % of cases [10•]. ATTR amyloidosis is divided in two subtypes: wild-type ATTR and hereditary/mutant ATTR. Wild-type ATTR, formerly known as senile systemic amyloidosis, is a

disease that predominantly affects the elderly. Although its true prevalence is unknown, postmortem studies revealed wild-type ATTR deposition in approximately 25 % of individuals 80 years and older [11]. In a majority of cases, the heart is the only affected organ and patients typically present with infiltrative cardiomyopathy and symptoms of heart failure [12]. Hereditary-ATTR is caused by mutations in the TTR gene leading to a less stable TTR protein and high tendency to forming amyloid fibrils. More than 100 different point mutations have been identified thus far [13–15]. Besides cardiomyopathy, patients with hereditary-ATTR usually develop

concurrent peripheral and autonomic neuropathy [16]. Cardiac involvement in all types of amyloidosis is a primary determinant of treatment selection and prognosis. Currently, the gold standard test for the diagnosis of cardiac amyloidosis (CA) is endomyocardial biopsy with immunohistochemical staining. However, due to the invasive nature of the procedure and the application of current advances in noninvasive imaging modalities, the diagnosis of CA is frequently obtained without endomyocardial biopsy. Current innovative advances in the use of noninvasive imaging for diagnosing CA is the primary focus of this review.

## Echocardiography

Echocardiography is the most utilized imaging modality for diagnosing CA. The echocardiographic features of CA, first illustrated on M-mode tracings in 1975, were described as a “stiff heart” with normal left ventricle (LV) diastolic dimensions, increased systolic dimension, and a small pericardial effusion [17]. When two-dimensional echocardiography was later introduced, cardiac amyloid phenotype was characterized further. This phenotype consists of a thick-walled ventricle with increased myocardial echogenicity giving it a speckled appearance [18, 19], valve thickening, small LV chamber volume, bi-atrial enlargement, small pericardial effusion, and restrictive diastolic filling [20]. LV systolic function is usually preserved in the early stages of the disease [19, 21, 22]. Increased ventricular wall thickening in the presence of electrocardiographic low-voltage was found to have a diagnostic sensitivity and specificity around 70 and 90 %, respectively [3, 23]. Although these findings are characteristic of AL CA, they are most often seen only in later stages of the disease [24]. Similar echocardiographic features are described in ATTR CA [25]. In the late 1980s, color flow Doppler provided a better understanding of the physiology of heart failure in CA and introduced diastolic dysfunction as a cardinal characteristic of this disease [26]. A study done by Klein et al. analyzed left ventricular inflow by Doppler proved that shortened deceleration time and increased early diastolic filling velocity to atrial filling velocity ratio were good predictors of cardiac death [27]. Recently, advanced echocardiographic techniques revealed further underlying mechanical abnormalities in CA and helped refine the approach to diagnosis and disease prognostication [28]. A decline in longitudinal function measured by strain and strain rate with tissue Doppler imaging detected early impairment in LV systolic function before alterations in conventional echocardiographic parameters or the onset of heart failure symptoms in CA [29–31]. Doppler-derived peak mean basal strain was also found to be a strong predictor of clinical outcome and superior to traditional echocardiographic parameters [32]. However, tissue Doppler based strain imaging has been surpassed by speckle-tracking echocardiography (STE), an angle-independent technique that has less intra and inter-observer variability. STE global longitudinal strain analysis differentiates CA from hypertrophic

cardiomyopathy and secondary LV hypertrophy [33]. Interestingly, in patients with AL and ATTR CA, regional longitudinal strain is significantly reduced in all segments in the mid-ventricle and basal wall regions but with apical sparing, see Fig. 1. This is demonstrated by a characteristic “polar map” plot seen in color-coded LV strain display. These findings are in contrast with hypertrophic cardiomyopathy in which regional longitudinal strain is markedly reduced at the septum [34•].

In regards to the echocardiographic differences among the most common types of amyloidosis, wild-type ATTR is characterized by greater LV wall thickness compared to hereditary-ATTR and AL amyloidosis [35]. Also, apical regional strain is significantly lower in ATTR when compared to AL amyloidosis [34•].

## Nuclear imaging

Multiple nuclear medicine imaging techniques and radiopharmaceuticals are available for the diagnosis and prognostication of CA. This review focuses on the three most studied and commonly used modalities; (Technetium-99m)-3,3-diphosphono-1,2-propanodicarboxylic acid (99mTc-DPD) scintigraphy, Iodine-123 Metaiodobenzylguanidine (I-123 MIBG) scan, and Pittsburgh compound-B labelled with the radionuclide carbon-11 (11C-PiB) positron emission tomography (PET).

## Bone-seeking tracers

99mTc-DPD is a non-FDA-approved bone-seeking tracer. Studies have consistently shown that patients with ATTR CA have a strong myocardial uptake of the tracer with statistically significant higher heart retention and heart to whole-body retention ratio (H/WB) of late 99mTc-DPD compared to AL CA patients

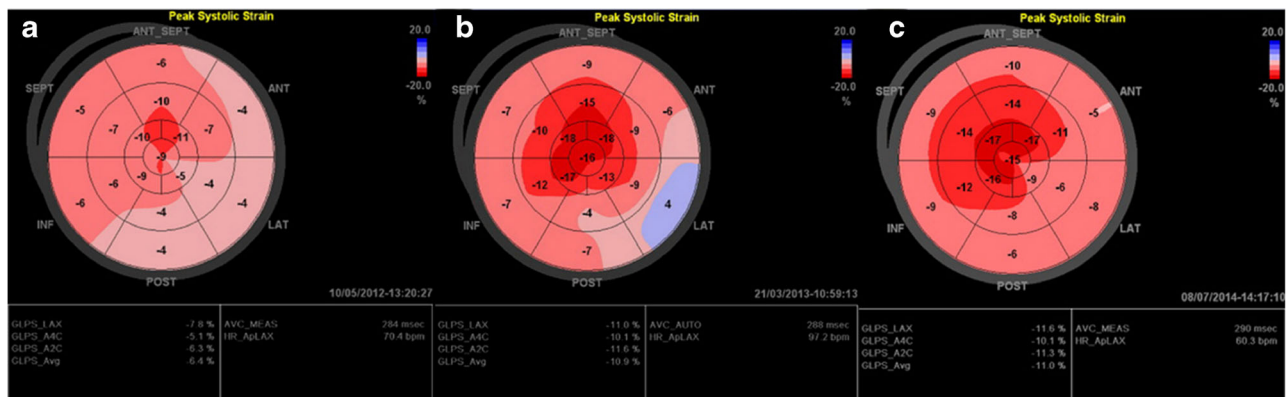


**Fig. 1.** Serial polar map images obtained with STE from a 54 y/o man with primary lambda light chain amyloidosis, that received Velcade plus dexamethasone induction therapy, followed by autologous stem cell transplantation (SCT). **a** Polar map (PM) representation pre SCT showing markedly reduced longitudinal strain values, with a slight advantage in function to the apical (center) segments; GLS -6.4 %, LVEF=43 %, 6-min walk: 300 m. **b** Same map now 3 months after SCT; GLS -10.9 %, LVEF=46 %, 6-min walk: 600 m. **c** The images 16 months after SCT; GLS -11 %, LVEF=50 %, by then the patient could do a short jog.

and patients without CA [36, 37, 38]. Thus, in terms of differentiating ATTR from AL etiology, <sup>99m</sup>Tc-DPD scintigraphy has a sensitivity and specificity close to 100 % in CA patients with moderate-to-high myocardial uptake [20, 21]. In patients with mild myocardial uptake, positive predictive (PPV) and negative predictive value (NPV) are 80 and 100 %, respectively. Whereas in patients with strong myocardial uptake with attenuated bone uptake, PPV and NPV are 100 and 68 %, respectively [21]. <sup>99m</sup>Tc-DPD myocardial uptake has also been reported in elderly patients with wild-type ATTR [39]. In a recent study, <sup>99m</sup>Tc-DPD scintigraphy was used to evaluate elderly patients admitted with heart failure with preserved ejection fraction (HFpEF). This diagnostic modality was able to detect wild-type ATTR in 13 % of cases of HFpEF, thus suggesting a potential role of <sup>99m</sup>Tc-DPD scintigraphy as a screening tool in elderly patients with HFpEF [40]. Early detection with <sup>99m</sup>Tc-DPD myocardial uptake has also been described in hereditary-ATTR CA caused by unusual genetic mutations (non-Val30Met) even before electrocardiographic and echocardiographic changes occur. Finally, H/WB determined by <sup>99m</sup>Tc-DPD scintigraphy was found to be a significant predictor of major adverse cardiac event (MACE)-free survival. When mean left ventricle wall thickness is >12 mm, the presence of a H/WB >7.5 was associated with poor MACE-free survival [41].

## Sympathetic innervation

I-123 MIBG is a radioactive catecholamine analogue that is taken up by the presynaptic neural endings of the cardiac sympathetic system and stored in granules [42]. Thus, nuclear imaging with I-123 MIBG is indirect and only occurs when there is sympathetic nerve destruction. In 1995, the first report of lack of I-123 MIBG myocardial activity in a patient with familial amyloidotic polyneuropathy (FAP) was published [43]. Further studies found that I-123 MIBG can detect myocardial adrenergic denervation in patients with hereditary-ATTR before the development of echocardiographic signs of CA [44, 45].

## PET scan

<sup>11</sup>C-PiB is a tracer derived from thioflavin T, an amyloid dye. This compound is used in PET scanning to visualize amyloid deposits in patients with CA. Multiple small studies showed that <sup>11</sup>C-PiB uptake was consistently increased in all patients with CA, but not seen in healthy controls [46, 47]. The sensitivity and specificity of <sup>11</sup>C-PiB PET scan for the diagnosis of CA was 87 % (95 % confidence interval [CI] 0.58 to 0.98) and 100 % (95 % CI 0.56 to 1.00), respectively. The diagnostic accuracy is 0.91 [29].

## Cardiovascular magnetic resonance

Cardiovascular magnetic resonance (CMR), specifically with late-gadolinium enhancement (LGE), is a very useful imaging modality that can differentiate CA from other etiologies of LV hypertrophy such as hypertension and hypertrophic cardiomyopathy [48]. In terms of diagnosing CA, this modality has a sensitivity of 80 % and a specificity of 94 %. Its PPV and NPV are 92 and 85 %, respectively

[49]. LGE was introduced by Saeed et al. in 1989 to identify infarcted myocardial tissue [50]. When given intravenously, gadolinium diffuses out of the capillaries into the interstitium because it does not penetrate intact cell membranes [51, 52]. LGE occurs when there is an enlarged interstitial space. This is due to slower distribution kinetics and a higher regional gadolinium concentration [53, 54]. This phenomenon is seen in CA secondary to abnormal deposit of beta-pleated fibrils in the interstitium. Standard LGE techniques require selecting an appropriate inversion time, to nullify signals from normal cardiac muscle and visualize endomyocardial amyloid deposition. Adequate LGE appreciation anchors on an accurate inversion time selection; thus, it is imperative to work with an experienced operator in CMR with LGE. Global subendocardial is the classical LGE pattern described in both AL and ATTR amyloidosis which matches amyloid distribution on histology. [55] In CA, CMR with LGE has prognostic implications as well. Maceira et al. found that gadolinium kinetics could predict mortality. In their study, parameters such as a fast blood gadolinium clearance, a low intramyocardial subepicardium-subendocardium T1 gradient, and a low subepicardial-blood T1 gradient reflect a higher amyloid burden and were associated with decreased survival. [56•] Myocardial T1 mapping is a CMR tissue characterization technique also used nowadays to diagnose CA. This technique uses native (without contrast) and post-contrast measurements, in addition to the patient's hematocrit, to determine myocardial extracellular volume (ECV) [57–59]. Native T1, myocardial mean ECV calculated at contrast equilibrium (ECVi), and 15-min post-bolus (ECVb) are significantly increased in CA. Upon multivariate analysis an ECVi >0.45 remained significantly associated with mortality (hazard ratio 4.41, 95 % CI 1.35–14.4;  $P=0.01$ ). [60] Recently, Fontana et al. studied CA using LGE with phase-sensitive inversion recovery (PSIR). This reconstitution technique removes the problematic operator-dependent inversion time selection, decreasing the potential for human error. In this particular study, amyloid deposition in the heart was found to be a continuum, accurately represented by three different LGE patterns (absent, subendocardial, and transmural). The LGE patterns were found to correlate with amyloid burden assessed per ECV by T1 mapping, in both AL and TTR amyloidosis. Transmural LGE was found to be a significant predictor of mortality, regardless of the amyloid type (hazard ratio 4.1, 95 % CI 1.3–13.1;  $P<0.05$ ) [61•].

Regarding CMR with LGE differences among the different types of amyloidosis, subendocardial LGE is more prevalent in AL when compared to ATTR amyloidosis. On the other hand, transmural LGE is more prevalent in ATTR [61•].

## Commentary

The presence of cardiac involvement in amyloidosis is associated with poor outcomes. This is partially due to the challenges of early disease detection, especially in patients without systemic involvement. However, if CA is a diagnostic consideration, newer noninvasive imaging tools aid in achieving a diagnosis perhaps without the need of an endomyocardial biopsy. Given the reproducibility reported so far, the availability and cost, it is reasonable to believe that the best initial diagnostic modality used should be speckled

tracking echocardiography imaging for strain analysis. Not only is this imaging modality safe to use in patients with kidney injury, it can also help differentiate CA from hypertrophic cardiomyopathy or hypertensive cardiomyopathy. STE strain analysis detects mild systolic function impairment before a decrease in LV ejection fraction. CMR is without a doubt the most accurate imaging modality. Newer techniques like T1 mapping and LGE by PSIR provide early detection and prognosis of CA. When distinguishing CA etiology, both STE and MRI with LGE provide clues to differentiate AL from ATTR. However,  $^{99m}\text{Tc}$ -DPD is the best test for this purpose and is safe for use in patients with kidney injury.

If the use of CMR with LGE per PSIR and T1 mapping becomes more readily available worldwide, physicians will be able to detect CA in very early stages, while still susceptible to disease-modifying therapies. Thus, we predict an increase in the prevalence of CA due to both an increase in the diagnosis of asymptomatic patients and an increase in survival. We believe the need for endomyocardial biopsy in order to diagnose CA will decrease significantly.

## Compliance with Ethical Standards

### Conflict of Interest

The authors declare that they have no conflicts of interest.

### Human and Animal Rights and Informed Consent

This article does not contain any studies with human or animal subjects performed by any of the authors.

## References and Recommended Reading

Papers of particular interest, published recently, have been highlighted as:

- Of importance

1. • Merlino G, Bellotti V. Molecular mechanisms of amyloidosis. *N Engl J Med*. 2003;349(6):583–96.
- A review of the pathogenesis of amyloidosis.
2. Yan SD, Zhu H, Zhu A, Golabek A, Du H, Roher A, et al. Receptor-dependent cell stress and amyloid accumulation in systemic amyloidosis. *Nat Med*. 2000;6(6):643–51.
3. Sousa MM, Du YS, Fernandes R, Guimaraes A, Stern D, Saraiva MJ. Familial amyloid polyneuropathy: receptor for advanced glycation end products-dependent triggering of neuronal inflammatory and apoptotic pathways. *J Neurosci*. 2001;21:7576–86.
4. Rogers J, Webster S, Lue LF, Brachova L, Civin WH, Emmerling M, et al. Inflammation and Alzheimer's disease pathogenesis. *Neurobiol Aging*. 1996;17:681–6.
5. Andersson K, Olofsson A, Nielsen EH, Svehag SE, Lundgren E. Only amyloidogenic intermediates of transthyretin induce apoptosis. *Biochem Biophys Res Commun*. 2002;294:309–14.
6. Walsh DM, Klyubin I, Fadeeva JV, Cullen WK, Anwyl R, Wolfe MS, et al. Naturally secreted oligomers of amyloid beta protein potently inhibit hippocampal long-term potentiation in vivo. *Nature*. 2002;416:535–9.
7. • Sipe JD, Benson MD, Buxbaum JN, Ikeda S, Merlino G, Saraiva MJ, et al. Nomenclature 2014: amyloid fibril proteins and clinical classification of the amyloidosis. *Amyloid*. 2014;21:221–4.
- An up-to-date description of the different amyloid proteins affecting animals and humans and their nomenclature.
8. Kyle RA, Linos A, Beard CM, Linke RP, Gertz MA, O'Fallon WM, et al. Incidence and natural history of primary systemic amyloidosis in Olmsted County, Minnesota, 1950 through 1989. *Blood*. 1992;79(7):1817–22.



9. Pinney JH, Smith CJ, Taube JB, Lachmann HJ, Venner CP, Gibbs SD, et al. Systemic amyloidosis in England: an epidemiological study. *Br J Haematol*. 2013;161:525–32.
  10. • Dubrey SW, Cha K, Anderson J, Chamarthi B, Reisinger J, Skinner M, et al. The clinical features of immunoglobulin light-chain (AL) amyloidosis with heart involvement. *QJM*. 1998;91(2):141–57.
- A review of 232 patients with AL cardiac amyloidosis.
11. Cornwell 3rd GG, Murdoch WL, Kyle RA, Westermarck P, Pitkänen P. Frequency and distribution of senile cardiovascular amyloid. A clinicopathologic correlation. *Am J Med*. 1983;75(4):618–23.
  12. Dubrey SW, Falk RH. Amyloid heart disease. *Br J Hosp Med (Lond)*. 2010;71(2):76–82.
  13. Ando Y, Nakamura M, Araki S. Transthyretin-related familial amyloidotic polyneuropathy. *Arch Neurol*. 2005;62(7):1057–62.
  14. Connors LH, Lim A, Prokaeva T, Roskens VA, Costello CE. Tabulation of human transthyretin (TTR) variants, 2003. *Amyloid*. 2003;10(3):160–84.
  15. Zhang F, Hu C, Dong Y, Lin MS, Liu J, Jiang X, et al. The impact of V30A mutation on transthyretin protein structural stability and cytotoxicity against neuroblastoma cells. *Arch Biochem Biophys*. 2013;535(2):120–7.
  16. Lachman HJ, Booth DR, Booth SE, et al. Misdiagnosis of hereditary amyloidosis as AL (primary) amyloidosis. *N Engl J Med*. 2002;346(23):1786–91.
  17. • Chew C, Ziady GM, Raphael MJ, Oakley CM. The functional defect in amyloid heart disease: the “stiff heart” syndrome. *Am J Cardiol*. 1975;36:438–44.
- First description of the echocardiographic features of cardiac amyloidosis.
18. Cueto-Garcia L, Tajik AJ, Kyle RA, Edwards WD, Greipp PR, Callahan JA, et al. Serial echocardiographic observations in patients with primary systemic amyloidosis: an introduction to the concept of early (asymptomatic) amyloid infiltration of the heart. *Mayo Clin Proc*. 1984;59(9):589–97.
  19. Rahman JE, Helou EF, Gelzer-Bell R, Thompson RE, Kuo C, Rodriguez ER, et al. Noninvasive diagnosis of biopsy-proven cardiac amyloidosis. *J Am Coll Cardiol*. 2004;43(3):410–5.
  20. Selvanayagam JB, Hawkins PN, Paul B, Myerson SG, Neubauer S. Evaluation and management of the cardiac amyloidosis. *J Am Coll Cardiol*. 2007;50(22):2101–10.
  21. Simons M, Isner JM. Assessment of relative sensitivities of noninvasive tests for cardiac amyloidosis in documented cardiac amyloidosis. *Am J Cardiol*. 1992;69:425–7.
  22. Klein AL, Hatle LK, Taliencio CP, Taylor CL, Kyle RA, Bailey KR, et al. Serial Doppler echocardiographic follow-up of left ventricular diastolic function in cardiac amyloidosis. *J Am Coll Cardiol*. 1990;16:1135–41.
  23. Carroll JD, Gaasch WH, McAdam KP. Amyloid cardiomyopathy: characterization by a distinctive voltage/mass relation. *Am J Cardiol*. 1982;49(1):9–13.
  24. Falk RH. Diagnosis and management of the cardiac amyloidoses. *Circulation*. 2005;112:2047–60.
  25. Ng B, Connors LH, Davidoff R, Skinner M, Falk RH. Senile systemic amyloidosis presenting with heart failure: a comparison with light chain-associated amyloidosis. *Arch Intern Med*. 2005;165(12):1425–9.
  26. Klein AL, Hatle LK, Burstow DJ, Seward JB, Kyle RA, Bailey KR, et al. Doppler characterization of left ventricular diastolic function in cardiac amyloidosis. *J Am Coll Cardiol*. 1989;13(5):1017–26.
  27. Klein AL, Hatle LK, Taliencio CP, Oh JK, Kyle RA, Gertz MA, et al. Prognostic significance of Doppler measures of diastolic function in cardiac amyloidosis. A Doppler echocardiography study. *Circulation*. 1991;83(3):808–16.
  28. Porciani MC, Cappelli F, Perfetto F, Ciaccheri M, Castelli G, Ricceri I, et al. Rotational mechanics of the left ventricle in AL amyloidosis. *Echocardiography*. 2010;27(9):1061–8.
  29. Koyama J, Ray-Sequin PA, Falk RH. Longitudinal myocardial function assessed by tissue velocity, strain, and strain rate tissue Doppler echocardiography in patients with AL (primary) cardiac amyloidosis. *Circulation*. 2003;107(19):2446–52.
  30. Ogiwara F, Koyama J, Ikeda S, Kinoshita O, Falk RH. Comparison of the strain Doppler echocardiographic features of familial amyloid polyneuropathy (FAP) and light-chain amyloidosis. *Am J Cardiol*. 2005;95(4):538–40.
  31. Bellavia D, Pellikka PA, Abraham TP, Al-Zahrani GB, Dispenzieri A, Oh JK, et al. Evidence of impaired left ventricular systolic function by Doppler myocardial imaging in patients with systemic amyloidosis and no evidence of cardiac involvement by standard two-dimensional and Doppler echocardiography. *Am J Cardiol*. 2008;101(7):1039–45.
  32. Koyama J, Falk RH. Prognostic significance of strain Doppler imaging in light-chain amyloidosis. *JACC Cardiovasc Imaging*. 2010;3(4):333–42.
  33. Sun JP, Stewart WJ, Yang XS, Donnell RO, Leon AR, Felner JM, et al. Differentiation of hypertrophic cardiomyopathy and cardiac amyloidosis from other causes of ventricular wall thickening by two-dimensional strain imaging echocardiography. *Am J Cardiol*. 2009;103(3):411–5.
  34. • Phelan D, Collier P, Thavendiranathan P, Popović ZB, Hanna M, Plana JC, et al. Relative apical sparing of longitudinal strain using two-dimensional speckle-tracking echocardiography is both sensitive and specific for the diagnosis of cardiac amyloidosis. *Heart*. 2012;98(19):1442–8.
- A study comparing patients with CA versus LV hypertrophy of multiple etiologies showed regional variations in longitudinal strain from base to apex can help recognizing CA.
35. Quarta CC, Solomon SD, Uraizee I, Kruger J, Longhi S, Ferlito M, et al. Left ventricular structure and function in transthyretin-related versus light-chain cardiac amyloidosis. *Circulation*. 2014;129(18):1840–9.

36. Puille M, Altland K, Linke RP, Steen-Muller MK, Kiett R, Steiner D, et al. <sup>99m</sup>Tc-DPD scintigraphy in transthyretin-related familial amyloidotic polyneuropathy. *Eur J Nucl Med Mol Imaging*. 2002;29(3):376–9.
37. • Perugini E, Guidalotti PL, Salvi F, Cooke RM, Pettinato C, Riva L, et al. Noninvasive etiologic diagnosis of cardiac amyloidosis using <sup>99m</sup>Tc-3,3-diphosphono-1,2-propanodicarboxylic acid scintigraphy. *J Am Coll Cardiol*. 2005;46(6):1076–84.
- This study shows the utility of Tc-99m-DPD scintigraphy in the workup to differentiate TTR versus AL etiology.
38. Rapezzi C, Quarta CC, Guidalotti PL, Longhi S, Pettinato C, Leone O, et al. Usefulness and limitations of <sup>99m</sup>Tc-3,3-diphosphono-1,2-propanodicarboxylic acid scintigraphy in the aetiological diagnosis of amyloidotic cardiomyopathy. *Eur J Nucl Med Mol Imaging*. 2011;38(3):470–8.
39. Longhi S, Guidalotti PL, Quarta CC, Gagliardi C, Milandri A, Lorenzini M, et al. Identification of TTR-related subclinical amyloidosis with <sup>99m</sup>Tc-DPD scintigraphy. *JACC Cardiovasc Imaging*. 2014;7(5):531–2.
40. González-López E, Gallego-Delgado M, Guzzo-Merello G, de Haro-Del Moral FJ, Cobo-Marcos M, Robles C, et al. Wild-type transthyretin amyloidosis as a cause of heart failure with preserved ejection fraction. *Eur Heart J*. 2015;36(38):2585–94.
41. Rapezzi C, Quarta CC, Guidalotti PL, Pettinato C, Fanti S, Leone O, et al. Role of (<sup>99m</sup>Tc)-DPD scintigraphy in diagnosis and prognosis of hereditary transthyretin-related cardiac amyloidosis. *JACC Cardiovasc Imaging*. 2011;4(6):659–70.
42. Wieland DM, Brown LE, Rogers WL, Worthington KC, Wu JL, Clinthorne NH, et al. Myocardial imaging with a radioiodinated norepinephrine storage analog. *J Nucl Med*. 1981;22(1):22–31.
43. Nakata T, Shimamoto K, Yonekura S, Kobayashi N, Sugiyama T, Imai K, et al. Cardiac sympathetic denervation in transthyretin-related familial amyloidotic polyneuropathy: detection with iodine-123-MIBG. *J Nucl Med*. 1995;36:1040–2.
44. Tanaka M, Hongo M, Kinoshita O, Takabayashi Y, Fujii T, Yazaki Y, et al. Iodine-123 metaiodobenzylguanidine scintigraphic assessment of myocardial sympathetic innervation in patients with familial amyloid polyneuropathy. *J Am Coll Cardiol*. 1997;29(1):168–74.
45. Noordzij W, Glaudemans AW, van Rheeën RW, Hazenberg BP, Tio RA, Dierckx RA, et al. (<sup>123</sup>I)-labelled metaiodobenzylguanidine for the evaluation of cardiac sympathetic denervation in early stage amyloidosis. *Eur J Nucl Med Mol Imaging*. 2012;39(10):1609–17.
46. Antoni G, Lubberink M, Estrada S, Axelsson J, Carlson K, Lindsjö L, et al. In vivo visualization of amyloid deposits in the heart with <sup>11</sup>C-PIB and PET. *J Nucl Med*. 2013;54(2):213–20.
47. Lee SP, Lee ES, Choi H, Im HJ, Koh Y, Lee MH, et al. <sup>11</sup>C-Pittsburgh B PET imaging in cardiac amyloidosis. *JACC Cardiovasc Imaging*. 2015;8(1):50–9.
48. Mahrholdt H, Wagner A, Judd RM, Sechtem U, Kim RJ. Delayed enhancement cardiovascular magnetic resonance assessment of non-ischaemic cardiomyopathies. *Eur Heart J*. 2005;26(15):1461–74.
49. Vogelsberg H, Mahrholdt H, Deluigi CC, Yilmaz A, Kispert EM, Greulich S, et al. Cardiovascular magnetic resonance in clinically suspected cardiac amyloidosis: noninvasive imaging compared to endomyocardial biopsy. *J Am Coll Cardiol*. 2008;51(10):1022–30.
50. Saeed M, Wagner S, Wendland MF, Derugin N, Finkbeiner WE, Higgins CB. Occlusive and reperfused myocardial infarcts: differentiation with Mn-DPDP—enhanced MR imaging. *Radiology*. 1989;172:59–64.
51. Wesbey GE, Higgins CB, McNamara MT, Engelstad BL, Lipton MJ, Sievers R, et al. Effect of gadolinium-DTPA on the magnetic relaxation times of normal and infarcted myocardium. *Radiology*. 1984;153:165–9.
52. Kim RJ, Chen EL, Lima JA, Judd RM. Myocardial gadolinium-DTPA kinetics determine MRI contrast enhancement and reflect the extent and severity of myocardial injury after acute reperfused infarction. *Circulation*. 1996;94:3318–26.
53. Flacke SJ, Fischer SE, Lorenz CH. Measurement of the gadopentetate dimeglumine partition coefficient in human myocardium in vivo: normal distribution and elevation in acute and chronic infarction. *Radiology*. 2001;218:703–10.
54. Kim RJ, Chen EL, Lima JA, Judd RM. Myocardial Gd-DTPA kinetics determine MRI contrast enhancement and reflect the extent and severity of myocardial injury after acute reperfused infarction. *Circulation*. 1996;94:3318–26.
55. Maceira AM, Joshi J, Prasad SK, Moon JC, Perugini E, Harding I, et al. Cardiovascular magnetic resonance in cardiac amyloidosis. *Circulation*. 2005;111(2):186–93.
56. • Maceira AM, Prasad SK, Hawkins PN, Roughton M, Pennell DJ. Cardiovascular magnetic resonance and prognosis in cardiac amyloidosis. *J Cardiovasc Magn Reson*. 2008;10:54.
- A study showing gadolinium kinetics can predict survival in patients with CA.
57. Flett AS, Hayward MP, Ashworth MT, Hansen MS, Taylor AM, Elliott PM, et al. Equilibrium contrast cardiovascular magnetic resonance for the measurement of diffuse myocardial fibrosis: preliminary validation in humans. *Circulation*. 2010;122:138–44.
58. Brooks J, Kramer CM, Salerno M. Markedly increased volume of distribution of gadolinium in cardiac amyloidosis demonstrated by T mapping. *J Magn Reson Imaging*. 2013;38:1591–5.
59. Mongeon FP, Jerosch-Herold M, Coelho-Filho OR, Blankstein R, Falk RH, Kwong RY. Quantification of extracellular matrix expansion by CMR in infiltrative heart disease. *JACC Cardiovasc Imaging*. 2012;5:897–907.



60. Banypersad SM, Fontana M, Maestrini V, Sado DM, Captur G, Petrie A, et al. T1 mapping and survival in systemic light-chain amyloidosis. *Eur Heart J*. 2015;36(4):244–51.
61. • Fontana M, Pica S, Reant P, Abdel-Gadir A, Treibel TA, Banypersad SM, et al. Prognostic value of late gadolinium enhancement cardiovascular magnetic resonance in cardiac amyloidosis. *Circulation*. 2015;132(16):1570–9.
- Largest CMR study in AL and ATTR patients showing PSIR technique is more accurate than standard techniques and amyloid deposition in the heart is a continuum.